

# A Tris-Cyclometalated Iridium(III) Complex of 2-(5,5-Dioxido-dibenzothiophen-3-yl)pyridine: Synthesis, Structural, Redox and Photophysical Properties

Mustafa Tavasli,<sup>[a]</sup> Sylvia Bettington,<sup>[a]</sup> Igor F. Perepichka,<sup>[a,b]</sup> Andrei S. Batsanov,<sup>[a]</sup> Martin R. Bryce,<sup>\*[a]</sup> Carsten Rothe,<sup>[c]</sup> and Andrew P. Monkman<sup>[c]</sup>

**Keywords:** Dibenzothiophene *S,S*-dioxide / Iridium / Cyclometalation / Luminescence / Electrochemistry

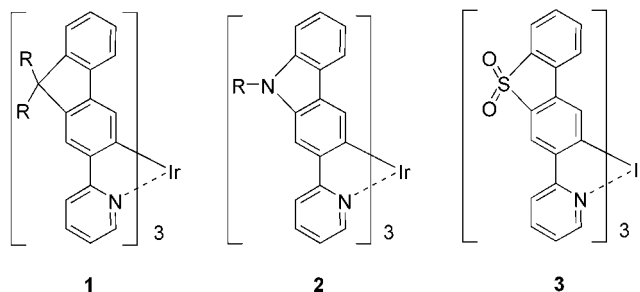
The first cyclometalated dibenzothiophene *S,S*-dioxide derivative, namely [*fac*-2-(5,5-dioxido-dibenzothiophen-3-yl)pyridine]iridium(III) (**3**) has been synthesised in high yield and characterised by X-ray crystallography, solution electrochemistry, absorption and emission spectroscopy. The Ir atom has a *fac*-octahedral coordination with three chelating ligands (*A*, *B* and *C*); each Ir–N bond is in *trans* position to an Ir–C bond. In cyclic voltammetry experiments in dichloromethane, complex **3** undergoes a reversible metal-centred Ir<sup>III</sup>/Ir<sup>IV</sup> oxidation at  $E_{1/2}^{ox} = +1.04$  V vs. Ag/Ag<sup>+</sup> reference electrode. Complex **3** exhibits bright green photoluminescence ( $\lambda_{max} = 525$  nm in toluene) from mixed <sup>3</sup>MLCT/<sup>3</sup> $\pi \rightarrow \pi^*$  states with quantum yield ( $\Phi_{PL}$ ) of 0.26 in toluene solution. The phosphorescence emission decay follows first order kinetics, with a lifetime of 4.9  $\mu$ s. A comparison of complex **3**

with analogues **1** and **2**, where the dibenzothiophene *S,S*-dioxide unit is replaced by 9,9-dihexylfluorene and *N*-hexylcarbazole respectively, establish that the substituent *para* to the Ir metal atom, i.e. CR<sub>2</sub> in **1**, NR in **2** and SO<sub>2</sub> in **3**, has a major influence on the redox and emission properties in this series. Organic light-emitting diodes (OLEDs) were fabricated by spin-coating techniques using a polyspirobifluorene copolymer (PSBF) as a host and complex **3** as dopant. In a single-layer blend configuration ITO/PEDOT:PSS/PSBF:3(8 wt.-%)/Ba/Al OLEDs showed pale blue/white light emission (CIE coordinates:  $x = 0.29$ ,  $y = 0.31$ ) arising from a combination of fluorescence from the host copolymer ( $\lambda_{max} = 450$  nm) and phosphorescence from **3** ( $\lambda_{max} = 530$  nm). (© Wiley-VCH Verlag GmbH & Co. KGaA, 69451 Weinheim, Germany, 2007)

## Introduction

Since Baldo et al.<sup>[1]</sup> first reported an organic light-emitting diode (OLED) with *fac*-tris(2-phenylpyridine)iridium [Ir(ppy)<sub>3</sub>] as an emitting guest in a blend with a host material, a variety of transition metal–ligand complexes have been studied from the viewpoint of their fundamental photophysical properties and for their optoelectronic applications. Mixing of the electrogenerated singlet and triplet excited states by intersystem crossing removes the spin-forbidden nature of the radiative relaxation of the triplet excited state so singlet and triplet excited states both contribute to light emission. Additionally, the triplet-state lifetime is shortened, thereby suppressing triplet–triplet annihilation. Particular emphasis has been placed on tris-cyclometalated *CN* iridium(III) complexes with their emission colours

spanning the blue, green and red regions.<sup>[2–5]</sup> Colour tuning in these complexes is achieved either by the peripheral functionalisation<sup>[2,3]</sup> of the parent 2-phenylpyridine with electron-withdrawing/donating substituents, or through variation of the cyclometalating ligands.<sup>[2,4]</sup> With regard to the latter, 2-(9,9-dialkylfluoren-2-yl)pyridine-based iridium(III) complexes **1** (alkyl = *n*-hexyl<sup>[6,7]</sup> or methyl<sup>[8]</sup>) and 2-(*N*-alkylcarbazol-2-yl)pyridine-based iridium(III) complexes **2** (alkyl = hexyl<sup>[9]</sup> or ethyl<sup>[10]</sup>) have been explored by us and others.



We were interested in incorporating a new unit, namely dibenzothiophene *S,S*-dioxide (DBThD), into the ligands of cyclometalated complexes. This moiety is of current interest in the field as linearly-conjugated co-oligomers and

[a] Department of Chemistry, Durham University, Durham DH1 3LE, United Kingdom  
Fax: +44-191-384-4737  
E-Mail: m.r.bryce@durham.ac.uk

[b] National Academy of Sciences of Ukraine, L. M. Litvinenko Institute of Physical Organic and Coal Chemistry, Donetsk 83114, Ukraine

[c] Department of Physics, Durham University, Durham DH1 3LE, United Kingdom

Supporting information for this article is available on the WWW under <http://www.eurjic.org> or from the author.

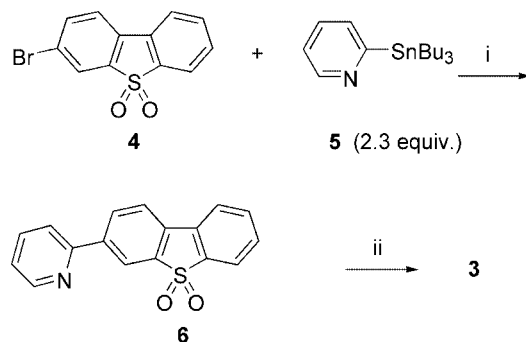
copolymers incorporating DBThD and 9,9-dialkylfluorene units are bright blue emitters in OLEDs, with the DBThD units imparting high stability, high fluorescence quantum yields and increased electron-transporting properties.<sup>[11,12]</sup> Other small-molecule DBThD derivatives have been used as an efficient electron-transporting layer (not the emitter) in OLEDs.<sup>[13]</sup>

We now report the synthesis of the first cyclometalated DBThD derivative, namely the *fac*-2-(5,5-dioxidodibenzothiophen-3-yl)pyridine iridium(III) complex (**3**), along with its structural, electrochemical and photophysical properties. Complex **3** is an analogue of complexes **1** and **2**, from which it differs in terms of the bridging group being SO<sub>2</sub>, instead of CR<sub>2</sub> in **1** or NR in **2**. These complexes constitute an interesting series for comparative redox and photophysical studies.

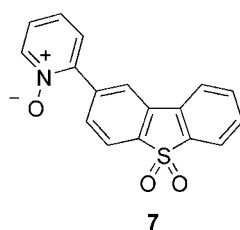
## Results and Discussion

### Synthesis

Ligand **6** was readily prepared by Stille<sup>[14]</sup> reaction of 3-bromodibenzothiophene *S,S*-dioxide **4**<sup>[15]</sup> with commercially available 2-tris(*n*-butyl)stannylpyridine (**5**)<sup>[16]</sup> in moderate yield (58%). An excess of ligand **6** was then treated with Ir(acac)<sub>3</sub> in glycerol at 220 °C<sup>[17]</sup> to give the *fac*-tris-cyclometalated iridium(III) complex **3** in 82% yield. The TGA analysis showed that complex **3** exhibits good thermal stability with a very high *T*<sub>d</sub> value of 490 °C (estimated at 5% weight loss temperature), which is ca. 75–100 °C higher than for complexes **1** and **2** and for Ir(ppy)<sub>3</sub>.<sup>[8]</sup> The synthesis and X-ray molecular structure of the related 2-(5,5-dioxidodibenzothiophen-2-yl)pyridine *N*-oxide (**7**) is given in the



Scheme 1. Reagents and conditions: i) Pd(PPh<sub>3</sub>)<sub>2</sub>Cl<sub>2</sub> (13% equiv.), toluene, 110 °C, 48 h (58% yield); ii) Ir(acac)<sub>3</sub>, glycerol, 220 °C, 48 h (82% yield).



Supporting Information (see footnote on the first page of this article). This compound was prepared during unsuccessful attempts to obtain an isomer of complex **3** (Scheme 1).

### X-ray Crystal Structures of Iridium Complex **3** and Its Precursor Ligand **6**

Crystallisation of **3** from CH<sub>2</sub>Cl<sub>2</sub>/MeOH yielded three pseudo-polymorphs, containing different (non-stoichiometric) amounts of disordered solvents, of which the triclinic form **3a** gave the most precise structure (Figure 1). The asymmetric unit comprises one molecule of **3** and an intermolecular void of ca. 80 Å<sup>3</sup> shared by a DCM molecule and a methanol molecule (modeled with occupancies 0.2 and 0.8, respectively), the latter hydrogen-bonded to a sulfone group. The Ir atom has a *fac*-octahedral coordination with three chelating ligands (*A*, *B* and *C*); each Ir–N bond is in a *trans* position to an Ir–C bond. Lengths of these bonds (Table 1) agree with X-ray studies of *fac*-Ir(ppy)<sub>3</sub><sup>[1b]</sup> and its derivatives.<sup>[6,18,19]</sup> The X-ray crystal structure of the free ligand **6** (Figure 2) revealed a practically planar molecule (except for the two oxygen atoms) with *cis* disposition of the N atom and the sulfone group. Upon coordination in complex **3**, the pyridine substituent adopts the opposite (*trans*) orientation, although the ligands are not entirely planar, as indicated by the dihedral angles between the pyridine ring and the two benzene rings (Table 1). Interestingly,

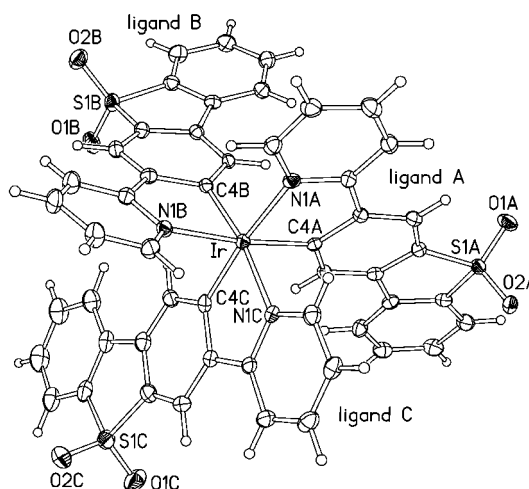


Figure 1. Molecule of **3** in the crystal of **3a** (50% thermal ellipsoids). For the atom and ring notation in the ligands see Figure 2.

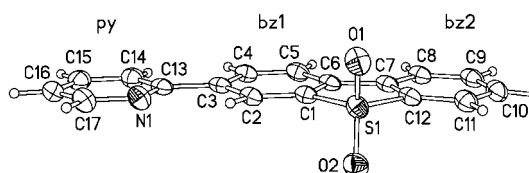


Figure 2. X-ray molecular structure of the free ligand **6** (50% thermal ellipsoids).

Table 1. Bond lengths [ $\text{\AA}$ ], bond and interplanar angles [ $^\circ$ ] in **3** and **6**.

Ligand	<b>6</b>	<b>3a</b> <i>A</i>	<b>3a</b> <i>B</i>	<b>3a</b> <i>C</i>	<b>3b</b> <i>A</i>
Ir–N		2.111(2)	2.130(2)	2.132(2)	2.101(9)
Ir–C(4)		2.005(3)	1.994(3)	2.017(3)	2.004(11)
N–C(13)	1.344(3)	1.369(3)	1.357(4)	1.375(3)	1.368(14)
N–C(17)	1.338(3)	1.347(3)	1.338(4)	1.343(4)	1.354(14)
C(3)–C(4)	1.404(3)	1.423(4)	1.427(4)	1.425(4)	1.451(16)
C(3)–C(13)	1.481(3)	1.474(4)	1.475(4)	1.464(4)	1.448(18)
C(4)–C(5)	1.387(3)	1.418(4)	1.411(4)	1.421(4)	1.361(15)
N–Ir–C(4)		79.7(1)	79.8(1)	79.9(1)	80.2(4)
py/bz1	1.9	5.3	15.2	6.3	3.2
py/bz2	2.0	6.3	28.6	7.4	3.1
bz1/bz2	0.7	4.5	13.4	2.5	1.0

Ligand	<b>3b</b> <i>B</i>	<b>3b</b> <i>C</i>	<b>3c</b> <i>A</i>	<b>3c</b> <i>B</i>	<b>3c</b> <i>C</i>
Ir–N	2.148(8)	2.092(9)	2.116(4)	2.134(3)	2.124(4)
Ir–C(4)	2.050(11)	2.010(10)	2.008(4)	2.010(4)	2.005(4)
N–C(13)	1.368(13)	1.353(15)	1.353(7)	1.361(5)	1.357(5)
N–C(17)	1.309(15)	1.378(15)	1.337(6)	1.352(5)	1.351(5)
C(3)–C(4)	1.453(14)	1.441(15)	1.428(6)	1.431(5)	1.428(5)
C(3)–C(13)	1.474(15)	1.457(17)	1.475(7)	1.464(6)	1.471(5)
C(4)–C(5)	1.362(15)	1.364(15)	1.406(6)	1.414(6)	1.408(5)
N–Ir–C(4)	81.1(4)	79.5(4)	79.71(17)	80.05(14)	79.98(14)
py/bz1	0.7	8.1	2.6	2.3	12.8
py/bz2	4.7	9.6	5.9	6.9	15.8
bz1/bz2	4.4	3.3	3.4	5.3	7.3

the looser is the molecular packing in a pseudo-polymorph of **3** (see the Experimental Section) the more planar are the ligands.

### Solution Electrochemical Properties

The cyclic voltammogram (CV) of complex **3** in dichloromethane displayed a reversible one-electron oxidation wave at  $E_{1/2}^{\text{ox}} = +1.04$  V vs.  $\text{Ag}/\text{Ag}^+$  reference (internal  $\text{Fc}/\text{Fc}^+$  reference gave  $+0.28$  V vs.  $\text{Ag}/\text{Ag}^+$  in these conditions). DFT calculations predict that dibenzothiophene *S,S*-dioxide has a LUMO energy level of 1.04 eV lower than that of 9,9-dialkylfluorene<sup>[11]</sup> and the substantial increase in oxidation potential of **3**, compared to complexes **1** and **2** ( $E_{1/2}^{\text{ox}} = +0.40$  V<sup>[7]</sup> and  $+0.14$  V,<sup>[9]</sup> respectively), indicates that the bridging  $\text{SO}_2$  group has dramatically reduced the electron density on the iridium centre. On the contrary, the carbazole nitrogen of **2** donates electron density to the Ir centre and hence the ease of oxidation in the series is **2** > **1** > **3**. Generally, oxidation processes which involve an Ir-aryl moiety are considered as a metal-centered couple,<sup>[20]</sup>

i.e.  $\text{Ir}^{\text{III}}/\text{Ir}^{\text{IV}+}$  in the present series. Similar to complexes **1** and **2**, complex **3** shows good chemical and electrochemical reversibility in CV experiments. The half-wave oxidation potentials ( $E_{1/2}^{\text{ox}}$ ) of the complexes **1**, **2** and **3** and ferrocene are summarised in Table 2; CV traces are shown in Figure 3.

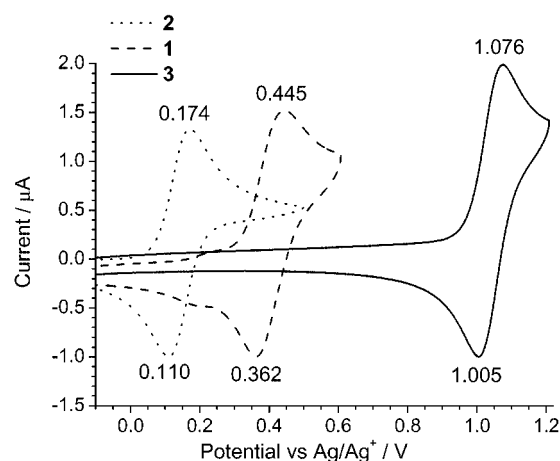


Figure 3. Cyclic voltammograms of complexes **1**, **2** and **3** in dichloromethane, electrolyte 0.1 M  $n\text{Bu}_4\text{NPF}_6$ , scan rate  $100 \text{ mV s}^{-1}$ .

Table 2. Summary of the half-wave oxidation potentials ( $E_{1/2}^{\text{ox}}/\text{V}$ ) obtained by cyclic voltammetry for complexes **1**, **2** and **3** and ferrocene (Fc) vs.  $\text{Ag}/\text{Ag}^+$  reference electrode.<sup>[a]</sup>

Compound	$E_{1/2}^{\text{ox}}$ (V) [ $\Delta E$ (mV)]
<b>1</b>	+0.40 [83]
<b>2</b>	+0.14 [64]
<b>3</b>	+1.04 [71]
Fc	+0.28 [70]

[a] Dichloromethane, 0.1 M  $n\text{Bu}_4\text{NPF}_6$ , scan rate =  $100 \text{ mV s}^{-1}$ ;  $\Delta E = E_{\text{pa}} - E_{\text{pc}}$ .

### Solution-State Photophysical Properties

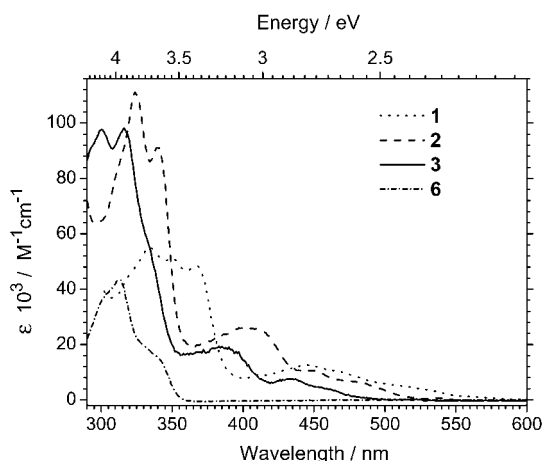
#### Absorption

The absorption spectrum of complex **3** in toluene solution is shown in Figure 4. Ligand **6** showed no absorption at all in the region of  $\lambda = 360$  to  $600 \text{ nm}$ ; for complex **3** the

Table 3. Absorption and emission spectra data for complexes **1**, **2**, and **3**, and ligand **6** in toluene.

Compound	Absorption, $\lambda_{\text{max}}$ (nm) [ $\epsilon$ (L mol <sup>-1</sup> cm <sup>-1</sup> )]	Emission, $\lambda_{\text{max}}$ (nm)
<b>1</b>	335 [55000], 350 [51000], 368 [48500], 445 [13500]	546, 583
<b>2</b>	313 sh [85000], 324 [111000], 340 [91000], 402 [26000], 448 [10500], 475 sh [6700]	587, 640 sh
<b>3</b>	300.5 [97500], 316 [98000], 331 sh [60000], 385 [19500], 434 [7500], 455 sh [4500]	525, 567, 610 sh
<b>6</b>	313 [43500], 330 sh [20000]	

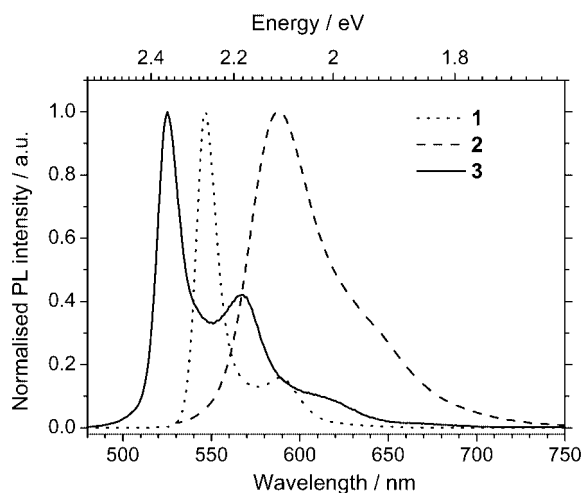
strong peaks below 360 nm are therefore assigned to spin-allowed ligand-centered  $^1\pi-\pi^*$  transitions, whereas the less intense absorption features seen above 360 nm are attributed to the metal-to-ligand charge-transfer (MLCT) transitions. As evident from their relative extinction coefficients, the absorption bands seen at around 385 nm and 450 nm are assigned to spin-allowed  $^1\text{MLCT}$  ( $\lambda = 385$  nm,  $\epsilon = 19500 \text{ M}^{-1} \text{ cm}^{-1}$ ) and spin-orbit coupling enhanced mixed  $^3\text{MLCT}$ - $^3\text{LC}$  ( $\lambda = 455$  sh nm,  $\epsilon \approx 4500 \text{ M}^{-1} \text{ cm}^{-1}$ ) transitions, respectively (Table 3). The whole spectrum of **3** is blue shifted compared to analogous fluorene and carbazole complexes **1**<sup>[7]</sup> and **2**,<sup>[9]</sup> indicating that the bridging  $\text{SO}_2$  group lowers the highest occupied molecular orbital (HOMO) energy level by withdrawing electrons from the system. These assignments were made on the basis of the literature data reported for other iridium complexes.<sup>[21]</sup>

Figure 4. The absorption spectra of ligand **6** and its complex **3** in toluene at room temperature. Spectra of analogous complexes **1** and **2** have also been shown for comparison.

### Emission

The photoluminescence (PL) spectrum of complex **3** obtained from degassed solutions in toluene (excitation at 400 nm) is shown in Figure 5, along with comparative spectra for **1** and **2**. The PL of complex **3** is characterised by a structured spectrum with two emission peaks around  $\lambda = 525$  and 567 nm (vibronic progression of  $1410 \text{ cm}^{-1}$ ) with a shoulder around  $\lambda = 610$  nm (Table 3). The highest energy emission peak is blue-shifted by ca. 21 nm and 62 nm from those of the complexes **1** ( $\lambda_{\text{em}} = 546$  nm)<sup>[7]</sup> and **2** ( $\lambda_{\text{em}} = 587$  nm),<sup>[9]</sup> respectively. The blue-shift in **3** is again attributed to the presence of  $\text{SO}_2$  group, which increases the HOMO–LUMO energy gap by withdrawing electrons from the iridium centre. The emission intensities, upon degassing,

increased without any change in the spectral profiles. Its sensitivity towards oxygen and long lifetime observed in the microsecond (4.9  $\mu\text{s}$ ) region both suggest that the emitting state has a triplet character.<sup>[22]</sup> The well-resolved vibronic structure, a large Stokes' shift (difference between the  $^3\text{MLCT}$  absorption and emission bands) and longer lifetime indicates that complex **3** emits from mixed  $^3\text{MLCT}/^3\pi\rightarrow\pi^*$  states, with a substantial  $^3\pi\rightarrow\pi^*$  contribution to the emitting states.<sup>[23]</sup>

Figure 5. Photoluminescence (PL) spectra for complex **3** (PL of analogous complexes **1** and **2** are also shown) in degassed toluene at room temperature,  $\lambda_{\text{ex}} = 400$  nm.

### Phosphorescence Lifetimes and Photoluminescence Quantum Yields

Time-resolved luminescence decay measurements for the complex **3** (OD < 0.1 at  $\lambda_{\text{ex}} = 355$  nm) were performed at 298 K in degassed toluene. The emission was collected at  $\lambda_{\text{max}}$  and the phosphorescence decay was found to follow first order kinetics, with a lifetime ( $\tau_p$ ) of 4.9  $\mu\text{s}$ . This lifetime is comparable with the values for **1** (2.8  $\mu\text{s}$ )<sup>[7]</sup> and **2** (3.2  $\mu\text{s}$ ).<sup>[9]</sup> The phosphorescent quantum yield ( $\Phi_{\text{PL}}$ ) of **3** is 0.26, measured at 298 K in thoroughly degassed toluene solution using  $\text{Ir}(\text{ppy})_3$  ( $\lambda_{\text{ex}} = 450$  nm,  $\Phi_{\text{PL}} = 0.40$  in toluene)<sup>[8,19]</sup> as the standard. This value is comparable with those for **1** ( $\Phi_{\text{PL}} = 0.24$ )<sup>[7]</sup> and **2** ( $\Phi_{\text{PL}} = 0.28$ ).<sup>[9]</sup>

### Organic Light Emitting Devices

Preliminary studies of OLEDs have been performed for single-layer devices with spin-coated PSBF:**3** layer, in the



following configuration: ITO/PEDOT:PSS/PSBF:3(8 wt.-%)/Ba/Al (PSBF is the host polyspirobifluorene copolymer; full details are given in the Supporting Information). Turn-on voltages were ca. 3 V. At driving voltages of 5–10 V, the diodes emit a pale blue/white light (CIE coordinates:  $x = 0.29$ ,  $y = 0.31$ ); the electroluminescence (EL) spectrum (Figure 6) demonstrates emission both from the host PSBF polymer around  $\lambda_{\text{max}} = 450$  nm and the characteristic emission of guest emitter (complex **3**) peaking at  $\lambda_{\text{max}} = 530$  nm. The latter phosphorescence is very similar in spectral shape to the emission spectrum of **3** in dilute solution (Figure 5) but is red shifted by ca. 5 nm in the devices. At ca.  $0.9 \times 10^6$  V cm<sup>-1</sup> the light output of the device reached a maximum of 300 cd/m<sup>2</sup>, which however, is accompanied by large currents, reducing the luminance efficiency to < 1 cd/A. Thus, both the luminance and the luminance efficiency are lower than complexes **1** (25000 cd/m<sup>2</sup> and 7.0 cd/A)<sup>[7]</sup> and **2** (4500 cd/m<sup>2</sup> and 1.7 cd/A).<sup>[9]</sup> The reason for this reduced performance of **3** is likely to be a combination of unbalanced charge injection and the inefficient excitation confinement at the guest emitter. Considering the latter, the triplet energies of both guest and host are of order of 2.3 eV.<sup>[24]</sup> Also, complex **3** has a high oxidation potential (HOMO level) compared to the other, better performing, complexes. Considering this, the holes may be less confined at the guest sites, implying that charge carrier recombination takes place at the host rather than the guest. This also explains the significant contribution of the host to the emission of the diode even at very low driving voltages. After exceeding ca. 0.9 V/cm the diode emission irreversibly changes from pale blue to orange with most of the host fluorescence now being quenched (Figure 6). At the same time, the guest emission becomes significantly broader and shifts to slightly lower energies. These simultaneous spectral changes indicate the formation of a new radiative site between guest emitter and host polymer.

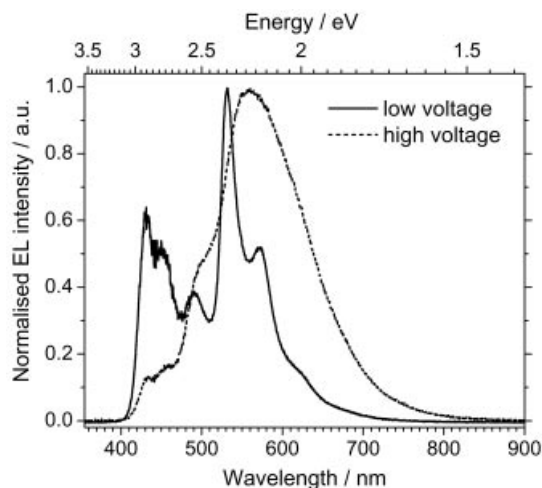


Figure 6. Electroluminescence (EL) spectrum of complex **3**, blended into polyspirobifluorene copolymer host. Device structure: ITO/PEDOT:PSS/PSBF:3(8 wt.-%)/Ba/Al. The spectra were taken at low (5 V) and high (15 V) applied voltage.

## Conclusions

The first cyclometalated dibenzothiophene *S,S*-dioxide derivative, namely *fac*-2-(5,5-dioxodibenzothiophen-3-yl)-pyridine iridium(III) **3** has been synthesised in high yield. The structure of the homoleptic CN Ir<sup>III</sup> complex **3** has been confirmed by X-ray crystallography. The complex exhibits good thermal stability with a very high  $T_d$  value of 490 °C. The electron-withdrawing DBThD unit, with its SO<sub>2</sub> unit *para* to the Ir centre, significantly raises the oxidation potential of complex **3** (Ir<sup>III</sup>/Ir<sup>IV</sup> transition;  $E_{1/2}^{\text{ox}} = +1.04$  V vs. Ag/Ag<sup>+</sup> reference) compared to the fluorene (**1**) and carbazole (**2**) analogs (+0.40 V and +0.14 V, respectively). Complex **3** displays green photoluminescence ( $\lambda_{\text{max}} = 525$  nm) attributed to mixed <sup>3</sup>MLCT/<sup>3</sup>π→π\* states, which is blue shifted compared to fluorene and carbazole complexes **1** and **2**. The phosphorescent quantum yield of **3** is  $\Phi_{\text{PL}} = 0.26$  in toluene solution; the decay followed first order kinetics, with a lifetime of 4.9 μs. Single-layer organic light-emitting diodes (OLEDs) were fabricated from a blend of complex **3** as a guest and polyspirobifluorene copolymer as a host demonstrated pale blue/white light emission (CIE coordinates:  $x = 0.29$ ,  $y = 0.31$ ) arising from a combination of fluorescence from the host copolymer ( $\lambda_{\text{max}} = 450$  nm) and phosphorescence from **3** ( $\lambda_{\text{max}} = 530$  nm). Future work will involve variations on the chemical structure of the 2-(5,5-dioxodibenzothiophen-3-yl)pyridine ligand to form new homoleptic and heteroleptic complexes, with the aim of tuning their photophysical properties, probing deeper into the fundamental properties of this fascinating class of materials and exploiting them as emitters in electrophosphorescent devices.

## Experimental Section

**2-(5,5-Dioxodibenzothiophen-3-yl)pyridine (6):** A mixture of 3-bromodibenzothiophene *S,S*-dioxide (**4**, 0.70 g, 2.73 mmol), LiCl (1.0 g, 22.5 mmol), 2-tris(*n*-butyl)stannylpyridine (**5**, 2.6 g, 6.36 mmol) and anhydrous toluene (50 mL) was placed in a flame-dried flask and purged with argon for 30 min at room temperature. Subsequently, [Pd(PPh<sub>3</sub>)<sub>2</sub>Cl<sub>2</sub>] (0.22 g, 13 mol.%) was added and the mixture was heated at 110 °C for 48 h. The warm reaction mixture was passed through a sinter and the remaining black residue was washed repeatedly (5 × 30 mL) with hot toluene. The combined filtrates were evaporated to dryness to give a pale orange solid. The crude product was column chromatographed [silica gel; eluent DCM to remove fast running impurities and then eluted with a mixture of DCM/EtOAc (95:5 v/v)] to give **6** which was finally washed with *n*-hexane to obtain a white solid (0.70 g, 58%),  $R_f = 0.74$  (EtOAc), m.p. 245–246 °C. <sup>1</sup>H NMR (500 MHz, CDCl<sub>3</sub>):  $\delta$  = 8.71 (d,  $J = 5.0$  Hz, 1 H), 8.44 (d,  $J = 1.5$  Hz, 1 H), 8.36 (dd,  $J = 6.0$  Hz, 1 H), 7.87 (d,  $J = 8.0$  Hz, 1 H), 7.84–7.76 (m, 4 H), 7.64 (td,  $J = 8.0$  Hz, 1 H), 7.53 (td,  $J = 7.5$  Hz, 2 H), 7.30 (m, 1 H) ppm. <sup>13</sup>C NMR (125 MHz, CDCl<sub>3</sub>):  $\delta$  = 155.0, 150.3, 142.0, 138.8, 138.5, 137.6, 134.3, 132.7, 132.2, 131.7, 130.8, 123.6, 122.6, 122.3, 122.2, 120.8, 117.3 ppm. MS (ES<sup>+</sup>):  $m/z = 294.2$  [M + H]<sup>+</sup>. C<sub>17</sub>H<sub>11</sub>NO<sub>2</sub>S·0.2H<sub>2</sub>O: calcd. C 68.76, H 3.87, N 4.72; found C 68.50, H 3.76, N 4.60. Crystals for X-ray analysis were grown from chloroform.

Table 4. Crystal data.

Compound	<b>3a</b>	<b>3b</b>	<b>3c</b>	<b>6</b>	<b>7</b>
CCDC number	645914	645915	645916	645913	645917
Formula	C <sub>51</sub> H <sub>30</sub> IrN <sub>3</sub> S <sub>3</sub> O <sub>6</sub> ·xCH <sub>2</sub> Cl <sub>2</sub> ·yMeOH			C <sub>17</sub> H <sub>11</sub> NO <sub>2</sub> S	C <sub>17</sub> H <sub>11</sub> NO <sub>3</sub> S
Solvent content <sup>[a]</sup>	x = 0.2, y = 0.8	x = 2, y = 2	x = 1, y = 3	—	—
Formula weight	1111.78	1303.10	1252.23	293.33	309.33
T [K]	120	120	120	120	120
Symmetry	triclinic	orthorhombic	orthorhombic	monoclinic	monoclinic
Space group	<i>P</i> $\bar{1}$ (# 2)	<i>Pbca</i> (# 61)	<i>Pbca</i> (# 61)	<i>P2<sub>1</sub>/c</i> (# 14)	<i>P2<sub>1</sub>/c</i> (# 14)
a [Å]	10.529(1)	19.189(2)	18.3159(14)	7.2777(8)	9.7017(9)
b [Å]	11.374(1)	11.558(1)	11.8180(8)	10.9635(10)	11.5570(11)
c [Å]	18.317(2)	45.717(5)	45.561(3)	16.5451(14)	12.4184(12)
$\alpha$ [°]	93.15(1)	90	90	90	90
$\beta$ [°]	92.41(1)	90	90	93.14(1)	103.945(10)
$\gamma$ [°]	91.81(1)	90	90	90	90
V [Å <sup>3</sup> ]	2187.1(4)	10140(2)	9862(1)	1318.1(2)	1351.3(2)
Z	2	8	8	4	4
$\mu$ [mm <sup>-1</sup> ]	3.28	3.03	3.01	0.25	0.25
Crystal size [mm]	0.15 × 0.14 × 0.06	0.32 × 0.24 × 0.08	0.51 × 0.26 × 0.11	0.49 × 0.07 × 0.05	0.25 × 0.20 × 0.10
Transmission	0.647–0.828	0.493–0.793	0.393–0.744	0.932–0.988	—
Reflections collected	27393	55652	107923	10612	14217
Unique reflections	12646, 10513 <sup>[b]</sup>	8894, 6309 <sup>[b]</sup>	14365, 11304 <sup>[b]</sup>	2319, 1730 <sup>[b]</sup>	3590, 2928 <sup>[b]</sup>
R <sub>int</sub> , %	5.0 (7.2 <sup>[c]</sup> )	7.5 (14.5 <sup>[c]</sup> )	7.7 (11.0 <sup>[c]</sup> )	7.1	4.7
R(F) <sup>[b]</sup> , wR(F <sup>2</sup> ), %	3.1, 6.3	8.3, 18.4	4.9, 9.8	3.7, 10.2	4.2, 10.3

[a] Tentative estimate, especially for **3b** and **3c**. [b] Reflections with  $I > 2\sigma(I)$ . [c] Before absorption correction.

**fac-2-(5,5-Dioxidodibenzothiophen-3-yl)pyridine Iridium(III) Complex (3):** A mixture of **6** (0.35 g, 1.19 mmol), Ir(acac)<sub>3</sub> (97%, 0.12 g, 0.23 mmol) and glycerol (10 mL) were heated to 220 °C under argon for 48 h. The mixture was cooled to room temperature and water (20 mL) was added. The suspension was extracted with DCM (4 × 30 mL) and the solvents evaporated to dryness giving an orange-brown solid. The crude material was column chromatographed [SiO<sub>2</sub>; eluent EtOAc, then toluene/EtOAc (8:2 v/v)] to give **3** as a bright orange solid (0.20 g, 82%), *R<sub>f</sub>* = 0.42 (EtOAc). M.p. ca. 230 °C (broad). <sup>1</sup>H NMR (500 MHz, CDCl<sub>3</sub>):  $\delta$  = 8.13 (s, 3 H), 8.04 (d, *J* = 8.0 Hz, 1 H), 7.83 (t, *J* = 5.0 Hz, 1 H), 7.77 (d, *J* = 8.0 Hz, 1 H), 7.50–7.47 (m, 2 H), 7.43–7.40 (m, 2 H), 7.32 (s, 1 H), 7.10 (t, *J* = 6.5 Hz, 1 H) ppm. <sup>13</sup>C NMR (125 MHz, CDCl<sub>3</sub>):  $\delta$  = 169.7, 164.1, 147.6, 146.3, 138.9, 138.2, 133.9, 132.6, 133.3, 131.2, 130.4, 129.3, 124.2, 122.8, 122.0, 120.4, 117.6 ppm. MALDI-ToF *m/z* = 1069.2 (M)<sup>+</sup>. C<sub>51</sub>H<sub>30</sub>IrN<sub>3</sub>O<sub>6</sub>S<sub>3</sub>H<sub>2</sub>O: calcd. C 56.34, H 2.97, N 3.86; found C 56.49, H 2.68, N 3.79. Single crystals for X-ray analysis were grown from a mixture of methanol and dichloromethane.

**X-ray Crystallography:** Single-crystal X-ray diffraction data were collected with Bruker 3-circle diffractometers with 1 K (for **3b**) or 6 K CCD area detectors, using graphite-monochromated Mo-*K $\alpha$*  radiation ( $\lambda$  = 0.71073 Å) and Cryostream (Oxford Cryosystems) open-flow N<sub>2</sub> cryostats, and corrected for absorption by numerical integration based on crystal face-indexing. The structures were solved by direct methods and refined by full-matrix least-squares against *F*<sup>2</sup> of all data, using SHELXTL software.<sup>[25]</sup> Crystal data and other experimental details are listed in Table 4. CCDC-645913 to -645917 contain the supplementary crystallographic data for this paper, which can be obtained free of charge from The Cambridge Crystallographic Data Centre via [www.ccdc.cam.ac.uk/data\\_request/cif](http://www.ccdc.cam.ac.uk/data_request/cif).

Crystallisations of **3** from DCM/MeOH produced three pseudo-polymorphs, always containing one molecule of the complex per asymmetric unit, but differing by the (non-stoichiometric) amounts of disordered solvents. In the triclinic form **3a** a closed intermo-

lecular void of ca. 80 Å<sup>3</sup> is shared by DCM and methanol molecules (with estimated occupancies of 0.2 and 0.8, respectively), so that the methyl carbon of the latter coincides with a chlorine atom of the former. The guest methanol is hydrogen-bonded to a sulfone group of **3**.

Two orthorhombic (space group *Pbca*) pseudo-polymorphs, **3b** and **3c**, crystallize in broadly similar unit cells with similar positions of the host molecules, which are packed in layers along the *z* = 0 and *z* = 1/2 planes, and leave in each unit cell four large voids, of ca. 630 Å<sup>3</sup> (**3b**) or 565 Å<sup>3</sup> (**3c**) each, filled with chaotically disordered solvents, for which no meaningful model could be found. The total volume of these voids amounts to ca. 25% and 23% of the crystal volume, respectively (cf. 7% in **3a**). From these volumes and the amount of residual electron density (much higher in **3b** than in **3c**) the compositions can be tentatively estimated as **3**·2CH<sub>2</sub>Cl<sub>2</sub>·2MeOH (**3b**) and **3**·CH<sub>2</sub>Cl<sub>2</sub>·3MeOH (**3c**). The crystallization of **3b** and **3c** in fact precedes that of **3a**, in agreement with Ostwald's rule of stages. The structures of **3b** and **3c** were refined using the back-Fourier transformation of the continuous density found in a masked region of the difference map,<sup>[26]</sup> to account for the missing solvent.

**Supporting Information** (see also the footnote on the first page of this article): General details of procedures and equipment used in this work. Chemical structure of the host PSBF copolymer used in the OLEDs. Detailed procedures for the synthesis of 2-(dibenzothiophen-2-yl)pyridine and 2-(5,5-dioxidodibenzothiophen-2-yl)pyridine *N*-oxide. X-ray crystal structure of 2-(5,5-dioxidodibenzothiophen-2-yl)pyridine *N*-oxide.

## Acknowledgments

We thank Durham County Council (Project SP/082), Cenamps (Newcastle upon Tyne, U.K.) and the University of Durham Photonic Materials Institute for funding this work.

[1] a) M. A. Baldo, S. Lamansky, P. E. Burrows, M. E. Thompson, S. R. Forrest, *Appl. Phys. Lett.* **1999**, 75, 4–6; b) For a structure

- determination of *fac*-Ir(ppy)<sub>3</sub> see: J. Breu, P. Stössel, S. Schrader, A. Starukhin, W. J. Finkenzeller, H. Yersin, *Chem. Mater.* **2005**, *17*, 1745–1752.
- [2] A. B. Tamayo, B. D. Alleyne, P. I. Djurovich, S. Lamansky, I. Tsyba, N. N. Ho, R. Bau, M. E. Thompson, *J. Am. Chem. Soc.* **2003**, *125*, 7377–7387.
- [3] a) R. Ragni, E. A. Plummer, K. Brunner, J. W. Hofstra, F. Babudri, G. M. Farinola, F. Naso, L. De Cola, *J. Mater. Chem.* **2006**, *16*, 1161–1170; b) V. V. Grushin, N. Herron, D. D. LeCloux, W. J. Marshall, V. A. Petrov, Y. Wang, *Chem. Commun.* **2001**, 1494–1495; c) T. Tsuzuki, N. Shirasawa, T. Suzuki, S. Tokito, *Adv. Mater.* **2003**, *15*, 1455–1458; d) K. Ono, M. Joho, K. Saito, M. Tomura, Y. Matsushita, S. Naka, H. Okada, H. Onnagawa, *Eur. J. Inorg. Chem.* **2006**, 3676–3683; e) A. S. Ionkin, W. J. Marshall, D. C. Roe, Y. Wang, *Dalton Trans.* **2006**, 2468–2478; f) J. Nishida, H. Echizen, T. Iwata, Y. Yamashita, *Chem. Lett.* **2005**, *34*, 1378–1379.
- [4] a) T. Sajoto, P. I. Djurovich, A. Tamayo, M. Yousufuddin, R. Bau, M. E. Thompson, *Inorg. Chem.* **2005**, *44*, 7992–8003; b) X. Zhang, C. Yang, L. Chen, K. Zhang, J. Qin, *Chem. Lett.* **2005**, *35*, 72–73; c) X. Zhang, J. Gao, C. Yang, L. Zhu, Z. Li, K. Zhang, J. Qin, H. You, D. Ma, *J. Organomet. Chem.* **2006**, *691*, 4312–4319.
- [5] Reviews: a) E. Holder, B. M. W. Langeveld, U. S. Schubert, *Adv. Mater.* **2005**, *17*, 1109–1121; b) P.-T. Chou, Y. Chi, *Chem. Eur. J.* **2007**, *13*, 380–395.
- [6] J. C. Ostrowski, M. R. Robinson, A. J. Heeger, G. C. Bazan, *Chem. Commun.* **2002**, 784–785.
- [7] M. Tavasli, S. Bettington, M. R. Bryce, H. A. Al Attar, F. B. Dias, S. King, A. P. Monkman, *J. Mater. Chem.* **2005**, *15*, 4963–4970.
- [8] A. Tsuboyama, H. Iwawaki, M. Furugori, T. Mukaide, J. Kamatani, S. Igawa, T. Moriyama, S. Miura, T. Takiguchi, S. Okada, M. Hoshino, K. Ueno, *J. Am. Chem. Soc.* **2003**, *125*, 12971–12979.
- [9] S. Bettington, M. Tavasli, M. R. Bryce, A. Beeby, H. Al-Attar, A. P. Monkman, *Chem. Eur. J.* **2007**, *13*, 1423–1431.
- [10] X. Zhang, C. Yang, L. Chen, K. Zhang, J. Qin, *Chem. Lett.* **2006**, *35*, 72–73.
- [11] I. I. Perepichka, I. F. Perepichka, M. R. Bryce, L.-O. Pålsson, *Chem. Commun.* **2005**, 3397–3399.
- [12] F. B. Dias, S. Pollock, G. Hedley, L.-O. Pålsson, A. Monkman, I. I. Perepichka, I. F. Perepichka, M. Tavasli, M. R. Bryce, *J. Phys. Chem. B* **2006**, *110*, 19329–19339.
- [13] T.-H. Huang, W.-T. Whang, J. Y. Shen, Y.-S. Wen, J. T. Lin, T.-H. Ke, L.-Y. Chen, C.-C. Wu, *Adv. Funct. Mater.* **2006**, *16*, 1449–1456.
- [14] Y. D. M. Champouret, R. K. Chaggar, I. Dadhiwala, J. Fawcett, G. A. Solan, *Tetrahedron* **2006**, *62*, 79–89.
- [15] I. I. Perepichka, I. F. Perepichka, M. R. Bryce, manuscript in preparation.
- [16] V. Fargeas, F. Favresse, D. Mathieu, I. Beaudet, P. Charrue, B. Lebre, M. Piteau, J.-P. Quintard, *Eur. J. Org. Chem.* **2003**, 1711–1721.
- [17] K. Dedeian, P. I. Djurovich, F. O. Garces, C. Carlson, R. J. Watts, *Inorg. Chem.* **1991**, *30*, 1685–1687.
- [18] F. O. Garces, K. Dedeian, N. L. Keder, R. J. Watt, *Acta Crystallogr., Sect. C* **1993**, *49*, 1117–1120.
- [19] S. Jung, Y. Kang, H.-S. Kim, Y.-H. Kim, C.-L. Lee, J.-J. Kim, S.-K. Lee, S.-K. Kwon, *Eur. J. Inorg. Chem.* **2004**, 3415–3423.
- [20] J. Brooks, Y. Babayan, S. Lamansky, P. I. Djurovich, I. Tsyba, R. Bau, M. E. Thompson, *Inorg. Chem.* **2002**, *41*, 3055–3066.
- [21] a) M. G. Colombo, T. C. Brunold, T. Riedener, H. U. Güdel, M. Fürtsch, H.-B. Bürgi, *Inorg. Chem.* **1994**, *33*, 545–550; b) S. Lamansky, P. Djurovich, D. Murphy, F. Abdel-Razzaq, R. Kwong, I. Tsyba, M. Bortz, B. Mui, R. Bau, M. E. Thompson, *Inorg. Chem.* **2001**, *40*, 1704–1711.
- [22] P. Coppo, E. A. Plummer, D. De Cola, *Chem. Commun.* **2004**, 1774–1775.
- [23] a) S. Lamansky, P. Djurovich, D. Murphy, F. Abdel-Razzaq, H.-E. Lee, C. Adachi, P. E. Burrows, S. R. Forrest, M. E. Thompson, *J. Am. Chem. Soc.* **2001**, *123*, 4304–4312; b) Y.-Y. Lyu, Y. Byun, O. Kwon, E. Han, W. S. Jeon, R. R. Das, K. Char, *J. Phys. Chem. B* **2006**, *110*, 10303–10314.
- [24] C. Rothe, S. King, A. P. Monkman, *Phys. Rev. B* **2006**, *73*, 245208-1/9.
- [25] *SHELXTL*, version 6.14; Bruker AXS, Madison, Wisconsin, U. S. A., **2003**.
- [26] P. van der Sluis, A. L. Spek, *Acta Crystallogr., Sect. A* **1990**, *46*, 194–201.

Received: June 4, 2007

Published Online: September 4, 2007